AIAA 2001-2961

The Rijke Tube Revisited via Laboratory and Numerical Experiments

J. Majdalani
Marquette University
Milwaukee, WI 53233

B. Entezam and W. K. Van Moorhem
University of Utah
Salt Lake City, UT 84112

35th AIAA Thermophysics Conference
11–14 June 2001
Anaheim, CA

The Rijke Tube Revisited via Laboratory and Numerical Experiments

J. Majdalani*
Marquette University, Milwaukee, WI 53233
and
B. Entezam† and W. K. Van Moorhem‡
University of Utah, Salt Lake City, UT 84112

In this paper, results proceeding from experimental studies and numerical simulations of the time-dependent flowfield inside a Rijke tube are presented and interpreted. A discussion is carried out based on existing speculations and standard scaling concepts. The main results include a similarity parameter that appears to play an important role in the heat driven oscillations. This parameter relates heat perturbations to velocity, pressure, and the square of a characteristic length. A hypothesis that relates heat oscillations to the compounded effects of pressure and velocity oscillations is discussed. This is done via computational, experimental, and scaling considerations. Since previous analytical theories have linked heat oscillations to *either* velocity or pressure coupling, the current analytical model agrees with and *reconciles between* both schools of thought. In compliance with the Rayleigh criterion, it is found that the heat source must be positioned at a critical distance of quarter length from the tube's entrance for resonance to occur. At that location, the modular product of acoustic velocity and pressure, known as the energy-flux vector modulus, is maximized. This observation confirms our proposed interpretation since the critical point where thermoacoustic coupling is maximized corresponds to the same spatial location where the modulus of acoustic intensity is largest. Furthermore, both numerical and laboratory experiments suggest that pressure oscillations inside the Rijke tube grow commensurately with increasing heat input. With a sufficiently small heat input, the acoustic sinks exceed the sources and acoustic attenuation takes place. In that case, no appreciable sound can be generated. Conversely, when the heat input is augmented beyond a critical threshold, acoustic sinks become insufficient, and rapid acoustic amplification ensues. The experiment also indicates the importance of the air's mean flow convection currents in the coupling mechanism. It is found that unless the air's mean flowrate is appreciable, no acoustic amplification can exist. To demonstrate the vitality of air currents, a strong mean flow is induced artificially by means of an exhaust fan. At the outset, acoustic growth is reported in both vertical and horizontal tube orientations. It is concluded that forced air currents can compensate for the lack of buoyancy in the horizontal tube configuration.

Nomenclature

a_0 = mean speed of sound inside the Rijke tube
A_{obs} = surface area of obstacle or heater element
C_p = constant pressure specific heat
h = heat transfer coefficient
$\bar{I}$ = acoustic intensity
L = internal tube length
m = longitudinal oscillation mode, $m = 1,2,3,...$
p' = oscillatory pressure component
Q = heat
q = heat transfer rate, dQ/dt
q' = oscillatory heat transfer rate
T = temperature
t = time
u' = oscillatory velocity component
V = volume

*Assistant Professor, Department of Mechanical and Industrial Engineering. Member AIAA.

†Research Scientist, Datum Corp., Irvine, CA. Member AIAA.

‡Professor, Department of Mechanical Engineering. Senior Member AIAA.

x = axial distance from the bottom-end
γ = mean ratio of specific heats
ρ = air density
ω = circular frequency, $m\pi a_0 / L$

Subscripts
obs = refers to the obstacle or heat source
∞ = surrounding mean flow condition
0 = denotes a steady or mean component

I. Introduction

THE fundamental mechanisms that arise in the Rijke tube have been adequately explained by several investigators. To that effect, one may cite the studies by Carrier,[1] Chu,[2] Miller et al.,[3] Maling,[4] Zinn,[5] and Raun et al.[6] The only aspect of the Rijke tube that is currently lacking full understanding lies in the detailed time-dependent interactions of the heat source and the acoustic flow that it induces. Such complex interactions occur in two banded regions that are separated by a diffuse interface delineating these two regions across the heat source. The resulting problem is not simple and requires careful attention, especially when the unsteady heat transfer at the boundaries is to be accounted for.

With these issues at hand, this investigation is carried out in an attempt to better explain the unsteady heat transfer mechanisms that cause the heat driven oscillations inside the Rijke tube. It is an extension to a previous study devoted entirely to the numerical simulation of the Rijke's internal field.[7] The reader is reminded that the phenomenon of heat driven acoustic oscillations belongs to the field of thermo-acoustics, a discipline that focuses on the interactions between heat and sound. In that context, whenever an unsteady heat source is enclosed in a chamber, the potential for heat-driven acoustic oscillations exists. Typically, high intensity sound pressure levels are generated by the incumbent acoustic oscillations in systems exhibiting a likeness to Rijke[8] or Soundhauss[9] tubes. Naturally, such consequences may or may not be desirable depending on the type of application.

Thermo-acoustic systems have been exploited in the past to perform beneficial functions in a number of industrial applications. Examples include: promoting higher combustion efficiency,[10-12] fuel savings,[13,14] controlled waste incineration,[15] slurry atomization,[16] reduced pollutant formation,[17-26] increased fuel residence time in combustion chambers,[27-29] increased convective heat transfer rates,[30] and lower operating and equipment costs.[13,31,32] The basic mechanisms that trigger the beneficial consequences are invariably associated with controlling the acoustic field[31] in order to improve mixing[33] and/or heat transfer.[14,34-37]

One of the archetypal applications of thermo-acoustics arises in the operation of coal-fired furnaces[14,20,28,31] and gas turbines.[6,35,38] In addition to its function in improving combustion efficiency, a pulsating pressure field is used to increase the size of exhaust particles. The reason is this. In the absence of user intervention, these particles usually escape along with the flue gases and contribute to air pollution. In fact, conventional removal methods allow over 70 percent of the particles (in the form of fine particulates) to escape and cause respiratory problems. Generally, particles smaller than about 5 microns are not efficiently removed. In trying to circumvent this deficiency, it has been demonstrated that acoustic energy is capable of promoting the agglomeration of fine ash particles entrained in high temperature gas streams.[11,12,17-21,24,26,29,39]

As the name suggests, acoustic agglomeration is a process in which high intensity sound is used to assemble micron and submicron sized particles in aerosols. The effect of sound is to cause relative motions between particles and increase their collision rate. As particles collide, they tend to bond and form larger particles. As a result, the average particle size in the aerosols increases in a short period of time. Evidently, the larger particles can be more effectively separated from exhaust gases by conventional particulate removal instruments. This has the beneficial effect of reducing particulate emissions and simplifying clean-up systems. Acoustic energy can also be employed to increase the rate and extent of coal combustion, allowing combustors to release larger amounts of heat.[14,35-37]

Contrary to their function in industrial applications, heat-driven oscillations in ramjet engines[40] and solid propellant rocket motors[41] are most undesirable. Corresponding thermoacoustic noise has often been named chugging, buzzing, screaming, screeching, or squealing, depending on its severity. These audible oscillations can cause unwanted vibrations plaguing instrumentation and payloads to the point of modifying rocket performance and throwing a missile off course.[41]

Due to the commonality of features in pulse combustion devices, the coupling aspects that we propose to investigate (inside a Rijke tube) may be present in a variety of problems incorporating heat, pressure and velocity perturbations.

The present analysis begins with a brisk description of pulse combustors, followed by a review of the fundamental concepts used to relate thermal fluctuations to acoustic pressure and velocity. A standard similarity analysis is used to disclose the dimensionless parameters that may be needed to establish a condition of similitude. The test apparatus is discussed and its results are used to verify both former and current speculations. The computational model is

later presented, followed by a discussion of experimental and numerical results. Numerical results are shown to be in accord with existing experimental and theoretical findings to the point of providing useful predictive tools. These tools tend to both clarify existing speculations and improve former analytical models.

II. Pulse Combustion

Pulse combustion differs from conventional combustion, where fuel is consummated under steady conditions, in the cyclical phenomena of the burning process.[28] The cyclic or oscillatory behavior can occur spontaneously or it can be triggered by an external device such as a spark plug or an acoustic driver. Pulsating combustion is achieved spontaneously when the heat released by the combustion process occurs at one of the system's natural frequencies. Acoustic wave interactions with the combustion process result in heat flux fluctuations. The strength of the coupling is contingent upon the magnitude of mean heat input within the system. For instance, at relatively low heat input, the coupling with the acoustic environment can be insignificant, due to small unsteady amplitudes. On the other hand, coupling at higher acoustic oscillation modes can require appreciably higher heat input. In order for the oscillations to persist, the rate at which heat is removed from the system must not exceed the rate at which acoustic heat energy is produced.

A. Governing Wave Equations

The wave equations with the heat addition term acting as a driving function can be written for acoustic pressure and velocity as follows[2]

$$\frac{1}{a_0^{\,2}}\frac{\partial^{\,2} p'}{\partial\, t^2} - \nabla^2 p' = \frac{1}{C_p T_0}\frac{\partial\, q'}{\partial\, t} \tag{1}$$

$$\frac{\partial^{\,2} u'}{\partial\, t^2} - a_0^{\,2}\ \nabla^2 u' = \frac{1-\gamma}{\rho_0}\frac{\partial\, q'}{\partial\, x} \tag{2}$$

Equations (1) and (2) are characteristic of self-excited or 'feedback' oscillations owing to the nature of the right-hand-side terms. Since the unsteady driving force q' that appears in Eqs. (1)–(2) is not externally controlled (but rather induced by fluctuations in other properties within the system), the Rijke tube is of the self-excited type.

By inspection of Eqs. (1)–(2), the presence of three unknown variables is noticed. The dependence of q' on the acoustic pressure and/or velocity must therefore be established if closure to the problem is desired. Proper auxiliary conditions in the vicinity of the heat source must also be expressed. Since no analytical formulation can ensue from Eqs. (1)–(2) without an additional equation that sets the model character, an appropriate relationship linking q' to p' and/or u' must precede further theoretical speculations. Such a relationship will be explored below. To begin, we review existing relationships that have been proposed in the past.

B. Pressure Coupling

Chu[2] assumes that, in thermoacoustical systems, the rate of heat addition is directly proportional to the rate of acoustic pressure, namely that

$$\frac{q'}{C_{p_0} T_0} = K\frac{\partial\, p'}{\partial\, t} \tag{3}$$

When used in Eq. (1), one obtains

$$\frac{1}{a_0^{\,2}}\frac{\partial^2 p'}{\partial t^2} - \nabla^2 p' = K\frac{\partial p'}{\partial t} \tag{4}$$

where the solution of Eq. (4) can be shown to be decaying for $K \le 0$, and growing for $K > 0$. Additionally, Chu suggests letting $K = \varepsilon\left(p_0^2 - p'^2\right)$ so that

$$\frac{1}{a_0^{\,2}}\frac{\partial^{\,2} p'}{\partial\, t^2} - \nabla^2 p' = \varepsilon\left(p_0^2 - p'^2\right)\frac{\partial\, p'}{\partial t} \tag{5}$$

This last equation describes self-sustained, large-amplitude pressure oscillations which increase until reaching steady limit-cycle oscillations. Chu's pressure coupling idea is useful to explain how heat and pressure oscillations are self-sustaining. However, it fails to explain the reason why no driving can occur at a velocity node despite maximum local pressure amplitudes. In addition, Eq. (4) does not satisfy Rayleigh's criterion which requires oscillation amplitudes to increase when

$$\oint q'p'\, dt > 0\,. \tag{6}$$

In Eq. (6), the symbol $\oint$ is used to denote integration over one oscillation cycle. Although Chu's assumption is valid for closed-open systems resembling the Soundhauss singing tube,[9] it does not quite apply to the Rijke tube.[8]

C. Velocity Coupling

Instead of attributing the coupling of heat oscillations to internal pressure fluctuations, another proposed relationship suggests that heat itself or velocity oscillations may stand behind the self-

sustained motion. In that context, Zinn[5,42] assumes that, for a combustion-driven Rijke tube, the heat transfer from the source to the gas depends on the magnitude of the total instantaneous velocity. Mathematically, this hypothesis translates into

$$q = C + a\left|u_0 + u'\right| = C + q_0 + q' \tag{7}$$

Here, C and a are constants, u_0 is the mean flow velocity, and u' is the acoustic velocity. This relationship appears to be an improvement over the previous formulation that attributes acoustic excitation to pressure coupling alone.

D. Energy Coupling

So far, we have reviewed two different expressions by Chu and Zinn relating heat oscillations to either pressure or velocity coupling via Eqs. (3) and (7). Our forthcoming results, however, have led us to suspect a different functional form. Before making headway or getting into details, we wish to bring the reader's attention to the prevalent symmetry in the coupled set given by Eqs. (1)–(2). This symmetry suggests that heat oscillations are more likely to be a function of both acoustic pressure and velocity, than a function of either one taken separately. At the outset, a possible relationship between q' and the product of the two acoustic quantities, p' and u' may have to be entertained. Physically, a symmetric expression can be constructed by positing a relationship between heat oscillations and the energy-flux vector modulus, $p'u'$. This proposed form will be further refined below.

III. Theoretical and Scaling Analysis

A. Theoretical Considerations

When heat is added to a volume of air, the air density diminishes. This causes an expansion of the volume occupied by the heated air. The periodic expansion and contraction of this volume produces pressure waves. These pressure waves can, in turn, influence the time-dependent thermal oscillations. Growing heat oscillation amplitudes are reported in the Rijke tube when the heat source is placed at a point where both acoustic pressure and velocity have additive amplitudes (see Fig. 1). Experimental observations also indicate that when the heat source is located at a distance of $\frac{1}{4}L$ from the bottom, the amplitude of pressure oscillations is maximized. This point corresponds to a maximum modular product of pressure and velocity. In order to reconcile between former theoretical speculations and existing observations, a relationship between acoustic heat, pressure, and velocity is suggested. This relationship has the form

$$q' \sim p'u'A \tag{8}$$

where A is the flow cross sectional area. In Eq. (8), the right-hand side, $p'u'$, is known as the energy-flux vector modulus. It represents the instantaneous energy flow per unit area for a given body of volume V. The time average of this vector is the acoustic intensity $\bar{\boldsymbol{I}}$. It is given by

$$\bar{\boldsymbol{I}} = \left\langle p'\boldsymbol{u}' \right\rangle = \frac{1}{\tau}\int_0^\tau p'\boldsymbol{u}'dt \tag{9}$$

where integration is carried out over an oscillation period τ. Since the acoustic energy $\bar{\boldsymbol{I}}$ has dimensions of power per unit area, the integral of $\bar{\boldsymbol{I}}$ over a surface with unit normal $\boldsymbol{n}$ is a measure of the acoustic power crossing that surface:

$$P = \int_A \left\langle p'\boldsymbol{u}' \cdot \boldsymbol{n}dA \right\rangle \tag{10}$$

From energy conservation, it is therefore reasonable to suggest that, this acoustic energy per unit time that crosses a given flow area, must originate from the thermal heat source energy, q'. A more refined

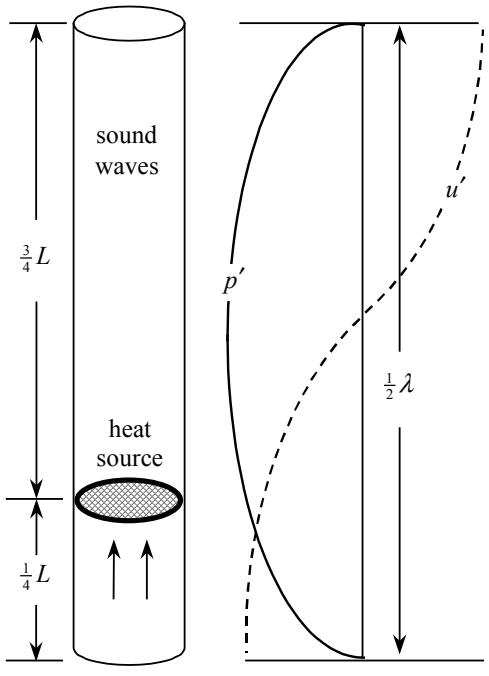

Fig. 1 The Rijke tube and its attendant acoustic character.

expression relating thermodynamic variables is hence proposed. This is

$$\langle q' \rangle \propto \int_A \langle p' \boldsymbol{u}' \cdot \boldsymbol{n} dA \rangle \tag{11}$$

For a mathematical model that is dominated by the longitudinal velocity component u' (in the direction of $\boldsymbol{n}$), Eq. (11) becomes

$$\langle q' \rangle \propto \int_A \langle p' u' dA \rangle \tag{12}$$

For a one-dimensional model, acoustic pressure and velocity are uniform along any cross-section. Thus one may write

$$\langle q' \rangle \propto \langle p' u' \rangle A \tag{13}$$

B. Scaling Considerations

Standard dimensional analysis can be used to determine the group parameters needed to establish a condition of similitude in the Rijke tube. Since computational fluid dynamics (CFD) and laboratory experimentation are both time-consuming and expensive, a practical goal here is to obtain the most information from the fewest experiments and/or computer runs.

To begin, we assume that heat oscillations can be influenced by variations in several variables. The most significant ones are: the pressure oscillation (p'), the velocity oscillation (u'), the temperature oscillation (T'), the temperature difference measured from heat source ($T_{\text{obs}} - T$), the heat source location (x_{obs}), the heat source diameter (d_{obs}), and the frequency of oscillations (f). In addition, we expect viscosity (μ), density (ρ), specific heat (C_p), heat transfer coefficient (h), speed of sound (a_0), tube length (L), and tube diameter (D) to be useful. The dependence of the dimensional heat oscillation on these parameters can be expressed as

$$q' = f\left(p', u', T', T_{\text{obs}} - T, x_{\text{obs}}, d_{\text{obs}}, f, \mu, \rho, C_p, h, a_0, L, D\right) \tag{14}$$

where the form of the function f is not yet known. After finding the rank of the dimensional matrix and applying the Buckingham-Pi theorem, one may choose $p', u', T',$ and D as repeating parameters. At the outset, 11 Pi parameters are obtained. These are:

$$\pi_1 = \frac{q'}{p' u' D^2};\ \pi_2 = \frac{\rho u'^2}{p'};\ \pi_3 = \frac{C_p T'}{u'^2};$$
$$\pi_4 = \frac{f D}{u'};\ \pi_5 = \frac{a_0}{u'};\ \pi_6 = \frac{h T'}{p' u'};\ \pi_7 = \frac{\mu u'}{p' D};$$
$$\pi_8 = \frac{x_{\text{obs}}}{D};\ \pi_9 = \frac{L}{D};\ \pi_{10} = \frac{d_{\text{obs}}}{D};\ \text{and}\ \pi_{11} = \frac{T_{\text{obs}} - T}{T'} \tag{15}$$

A simple rearrangement yields

$$\Pi_1 = F\left(\Pi_2, \Pi_3, \Pi_4, \Pi_5, \Pi_6, \Pi_7, \Pi_8, \Pi_9, \Pi_{10}, \Pi_{11}\right)$$

or

$$\frac{q'}{p' u' D^2} = F\left[\frac{p - p_0}{\rho u'^2}, \frac{\rho u'^2}{\rho C_p T'}, \frac{f L}{a_0}, \frac{u'}{a_0}, \frac{h(T_{\text{obs}} - T)}{p' u'}, \frac{\mu \frac{u'}{D}}{p'}, \frac{x_{\text{obs}}}{L}, \frac{L}{D}, \frac{d_{\text{obs}}}{D}, \frac{T'}{T_{\text{obs}} - T}\right] \tag{16}$$

Aside from the geometric scaling ratios, the following groups may be identified:

a) $\Pi_1 = \frac{q'}{p' u' D^2}$ is a similarity parameter that relates the fluctuating heat flux to acoustic pressure and velocity.

b) $\Pi_2 = \frac{p - p_0}{\rho u'^2} = E_u'$ is the ratio of fluctuating thermodynamic and dynamic pressures associated with the acoustic field. It is an expression of the unsteady Euler number.

c) $\Pi_3 = \frac{\rho u'^2}{\rho C_p T'}$ is the ratio of the dynamic pressure and the enthalpy of the acoustic field. This parameter can also be written alternatively, by using π_{11}, as $\frac{u'^2}{C_p (T_{\text{obs}} - T)} = E_c'$. The unsteady Eckert number that emerges is a measure of the unsteady kinetic energy per unit sensible enthalpy.

d) $\Pi_4 = f L / a_0 \sim m$ is the acoustic oscillation mode number. Recalling that, for an open tube, the frequency is given by $f = m a_0 / 2L$, this dimensionless ratio is equal to $m/2$.

e) $\Pi_5 = u' / a_0 = M'$ is the unsteady Mach number.

f) $\Pi_6 = \frac{q'}{h' D^2 (T_{\text{obs}} - T)} \sim 1$ is the ratio of the fluctuating heat flux and the unsteady convected heat. According to Newton's cooling law, this ratio should be constant.

g) $\Pi_7 = \frac{\mu u'}{p' D} \sim \frac{\mu\, du'/dr}{p'}$ is a measure of the unsteady viscous shear relative to the acoustic pressure.

h) $\Pi_{11} = \dfrac{T'}{T_{\text{obs}} - T} = \theta'$ is the dimensionless temperature.

At length, Eq. (16) reduces to

$$\frac{q'}{p'u'D^2} = F\left(E_u', E_c', m, M', \frac{\mu u'}{p'D}, \frac{x_{\text{obs}}}{L}, \frac{L}{D}, \frac{d_{\text{obs}}}{D}, \theta' \right) \quad (17)$$

Note that Π_1 is in agreement with the proposed form posited in Sec. III(A).

IV. Experimental Setup

A schematic of the Rijke tube employed in the experimental part of this study is shown in Fig. 2. The set-up is designed to have a simple cylindrical geometry that can be easily retrofitted when needed.

The simulated Rijke tube apparatus consists of several interchangeable, modular, two-inch nominal steel nipples. These interchangeable nipples are then joined together by three-way tees. The smaller side of the tee is connected to a short nipple, a reducer, a standard nipple, and a cap for inserting a microphone.

The tube is clamped either vertically or horizontally. The total length of the tube can be changed by replacing the nipples with either shorter or longer sections. Due to the isobaric openings on both ends, the length of the tube is half the oscillation wavelength.

After introducing the heat source, the magnitude of pressure oscillations and their frequency are measured at four different locations along the tube. This is done by inserting Realistic microphones into the tees and connecting them to a two-channel HP-3582A spectrum analyzer. To protect each microphone from the high pressures and temperatures inside the tube, the microphone tips are inserted perpendicularly to the tube into the 6" long nipples rather than directly into the tube. This is done in order to 1) avoid introducing vortex shedding around the microphone tip,[27] 2) reduce interference with measurements, and 3) provide a positive seal that prevents flow leakage past the microphone.

V. The Computational Model

The unsteady flowfield inside the Rijke tube has been computed with axisymmetric coordinates using a Navier-Stokes solver based on the Volume of Fluid (VOF) technique. This technique was first introduced by Hirt and Nichols in 1981.[43] The VOF method consists of three ingredients: a scheme to locate the surface, an algorithm to track the surface as a sharp interface moving through a computational grid, and a means of applying boundary conditions at the surface.[44]

In the computational model, the pipe is 90 centimeters in length and has an internal diameter of 5 centimeters. Only one cross section of the pipe is modeled, thus taking advantage of prevalent geometric symmetry. Evidently, since the pipe is a body of revolution, material properties, boundary conditions and other effects may be assumed to be symmetric with respect to the centerline.

The computational mesh for the domain representing half of the Rijke tube and room in the *r*–*x* directions is shown in Fig. 3. A solid porous obstacle with a diameter of 3.75 cm is added inside the tube at a location of 22.5 cm from the bottom-end. This obstacle is intended to model the physical heat source. An

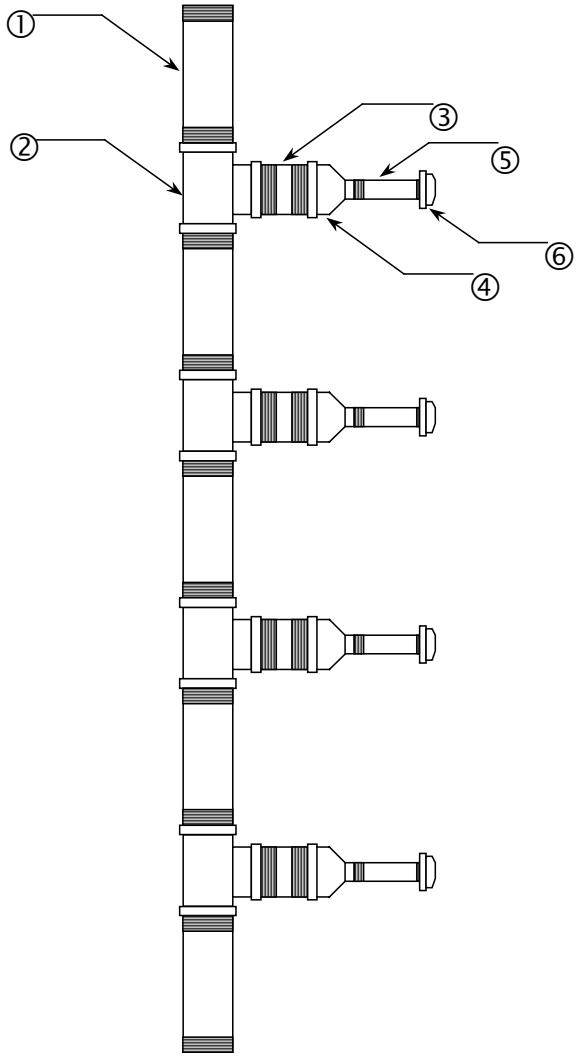

Fig. 2 Schematic diagram of the experimental apparatus. Items denote 1) nipple section (2 nominal), 2) tee section (2×2×½), 3) short nipple (½ nominal), 4) reducer (½×¼), 5) long nipple (¼×12), and 6) cap (¼). Dimensions are in inches.

obstacle porosity value of 0.9 is used to represent a 90 percent open area fraction. The thermal conductivity, density, and heat capacity of steel are used for obstacle properties. Heat is released inside the obstacle in a finite time step since releasing the heat suddenly causes a numerical singularity that can force the program to crash.

A. Heat Transfer Coefficients

Quasi-steady approximations of heat transfer coefficients are evaluated automatically by the code using standard correlations appropriate of heat convection from flat surfaces. The correlations implemented are based on four physical situations: natural convection, forced laminar convection, forced turbulent convection, and conduction within the fluid. All correlations are evaluated and the largest value is automatically selected by the program.

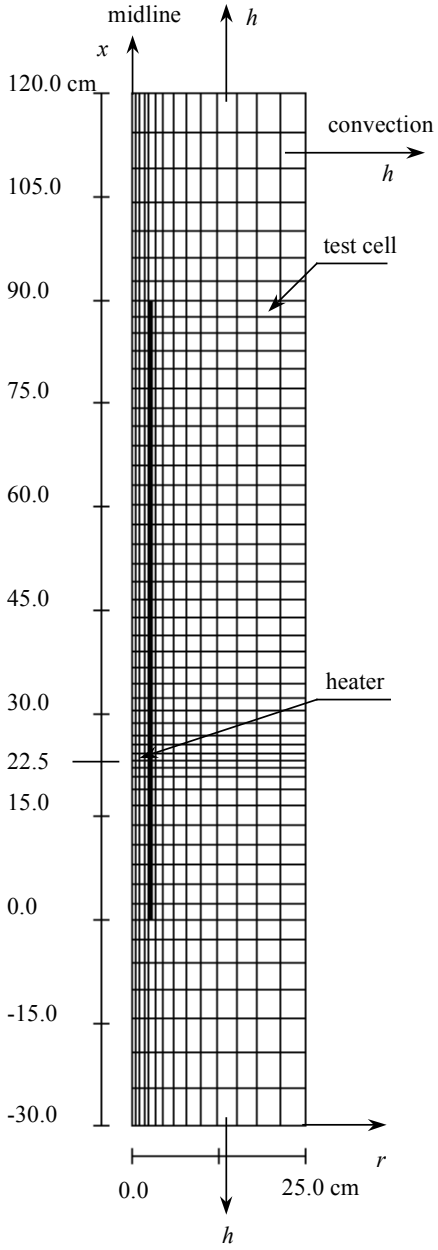

Fig. 3 Computational mesh.

B. Numerical Strategy

The numerical procedure evolves in two stages that are analogous to transient and steady-state solution phases. The first stage carries the problem from an initial state of rest to a time of 20 seconds. Subsequently, our problem exhibits limit-cycle oscillations that are characterized by nearly constant amplitudes.

The second stage hence carries the problem from 20 to 20.025 seconds with a much smaller time interval. This is done in order to track more precisely the progressive acoustic wave growth. Meanwhile, virtual probes are located inside the simulated tube at several axial locations. Numerically obtained pressures, temperatures, densities and velocities are thus acquired and tabulated.

VI. Results and Discussion

A. Experimental Results

The source (here, a Bunsen burner) is mounted vertically inside the lower half of the tube. The Bunsen burner heats the air around it and establishes a steady buoyancy-driven flow. The flame is moved back and forth to locate the optimal position that excites more effectively the system's natural frequency. The level of acoustic growth is measured using a soundmeter. As the flame is displaced, a loud and relatively pure tone is emitted and recorded by the microphones. This loud tone is continuously produced as long as energy is supplied at the heater. It is maximum when the heater is at $\frac{1}{4}L$ from the bottom.

Acoustic oscillations diminish noticeably when the outflow area at the top is reduced or obstructed. This can be attributed to two reasons. First, by constricting the outlet of the pipe, equal and opposite (mirror) waves are produced that reflect back and forth. This motion reduces the amplitude of acoustic oscillations. Second, by constricting the downstream end, the amount of air movement inside the tube is suppressed. This limits the convection heat transfer coefficient and reduces the acoustico-thermal mode coupling.

A separate test is used to verify that coupling with the naturally convected air flow is indeed a contributing factor to acoustic wave growth. This is accomplished by augmenting the air flowrate externally by means of a blower. When this is done, a higher intensity tone is emitted. Thus we come to realize that forcing the air

through the tube enhances the heat transfer coefficient and leads to a stronger acoustic environment.

The same experimental verification was conducted in a Rijke tube held horizontally. Initially, using the standard procedure and configuration, oscillations did not occur when the tube was horizontal. This was attributed to the absence of natural convection, an important contributing factor to the coupling with the acoustic waves. However, by adding a separate blower that forces air circulation, a strong convective motion was induced that was accompanied by a loud tone.

Some experimental results are displayed in Fig. 4 where the sound pressure amplitudes (SPL) are given for four different microphone locations along the pipe. In all cases, heat addition is applied approximately at $\frac{1}{4}L$ from the bottom. Results are also summarized in Table 1. Since the maximum acoustic pressure amplitude occurs in the middle and is zero at the open ends, the maximum SPL is recorded by the microphones that are closest to $x = \frac{1}{2}L$.

In these runs only the fundamental mode is excited at a frequency of approximately 250 Hz. This frequency corresponds to the finite length of the tube (L = 90 cm). The small variations in frequency are due to the temperature fluctuations inside the tube during the test. A slight movement of the heat source either downward or upward causes the amplitude to decrease. When the heat source is moved down to the $x = \frac{1}{8}L$ position, the second mode (f = 500 Hz) is observed along with the first. This is in complete agreement with Carvalho's experimental finding.[45] By the same token, moving the gauze to $x = \frac{1}{16}L$ triggers the first three oscillation modes.

B. Computational Results

Figure 5 is a graphical representation of the pressure, axial velocity, and source heat transfer rate for the first 20 seconds. It shows that, after about 8.5 seconds, heat, pressure, and velocity oscillations begin. At this point in time, the temperature at the source would have reached its limit-cycle condition characterized by constant amplitude oscillations (not shown). Since the establishment of thermal fluctuations must necessarily precede the inception of strong pressure waves, the role of thermal oscillations in driving the acoustic motion is clearly indicated.

Following the first 20 seconds, Fig. 6 shows the pressure, axial velocity, and source to fluid heat transfer during the second stage. Here, a smaller time step is used to track the acoustic wave growth more accurately. This figure indicates that periodic oscillations are

Table 1. Pressure amplitude at different locations along the Rijke tube

Microphone (Distance from the top -cm)	SPL (dB)	Prms (Pa)	Frequency (Hz)
65	134.5	108.3	248
55	135.7	124.3	254
35	135.6	122.9	246
25	132.5	86.0	260

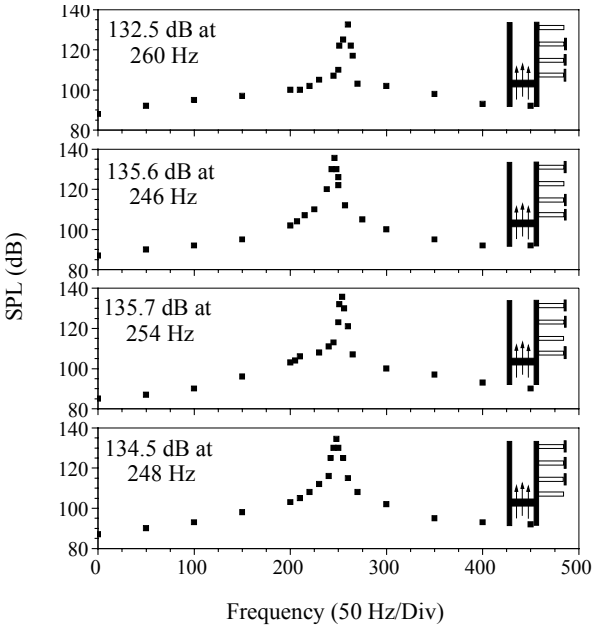

Fig. 4 Experimentally measured sound in the Rijke tube. From top to bottom, the microphone is located at 25, 35, 55, and 65 cm from the top. The inset indicates the location of the microphone.

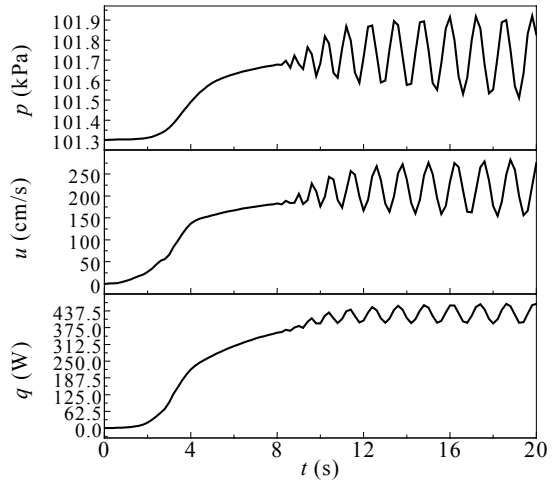

Fig. 5 Pressure, axial velocity and heat transfer for the first 20.0 seconds. This is a standard run with 430 watts supplied to the heater at $z = \frac{1}{4}L$.

present in all the variables with a frequency of about 200 Hz. This frequency matches the predicted natural frequency of the pipe, $f = ma_0/(2L)$. The result is reassuring and indicates that the numerical results are in accord with acoustic theory.

As explained in detail by Entezam, Van Moorhem and Majdalani,[7] it is found that a threshold for heat input intensity must be exceeded before any appreciable acoustic coupling can be seen. The phase angle between acoustic pressure and fluctuating heat flux is also found to be 45 degrees. The most significant result reported previously was the verification that maximum acoustic growth occurs when the energy heat flux vector is maximized.

As expected, the location of the source is found to be a key factor in producing thermoacoustic oscillations. When the source is placed in the lower half of the pipe, large amplitude oscillations are reported. The resulting oscillations are found to have the largest amplitudes when the source is located at precisely $\frac{1}{4}L$ from the bottom. During separate runs, the source was relocated to the middle ($\frac{1}{2}L$) and upper section ($\frac{2}{3}L$) of the pipe in order to observe whether or not the oscillations would occur.

The numerical results indicate that when the source is positioned at $\frac{1}{2}L$, the presence of an acoustic velocity node precludes the onset of oscillations. This observation is in agreement with the arguments presented in Sec. III. The latter, let us recall, predict zero acoustic intensity at the chamber's mid-point. By the same token, a very weak signal is recorded when the source is placed at $\frac{2}{3}L$. At that point, the oscillatory velocity and pressure are out of phase. As a result, their potential to trigger acoustic excitation is significantly diminished.

As determined previously by Entezam, Van Moorhem and Majdalani,[7] the pressure oscillations grow progressively with increasing heat input. It appears to be a minimum value of heat addition below which the thermoacoustic coupling is too weak to trigger any appreciable acoustic growth. With small heat input, the acoustic sinks exceed the sources and acoustic attenuation prevails. Conversely, when the heat input is augmented beyond a critical threshold, acoustic sinks become insufficient and rapid acoustic amplification takes place. In our numerical simulation, this critical value is observed for a heater power supply of approximately 430 watts.

The computational work also shows that the modulus of heat transfer oscillations is of the same order as the modular product of acoustic velocity amplitude, acoustic pressure amplitude, and the area of

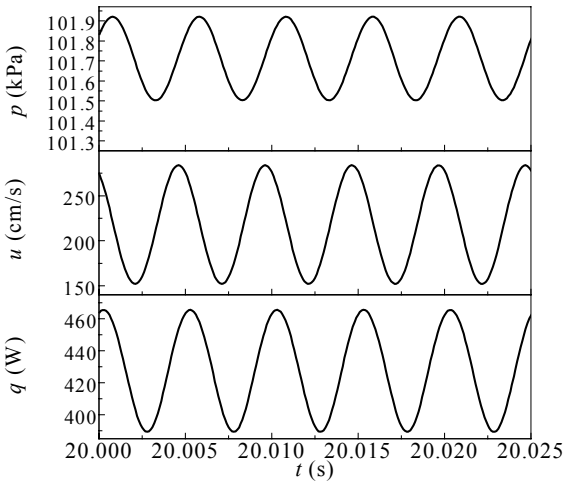

Fig. 6 Pressure, axial velocity and heat transfer using a time step of 0.0025 seconds during limit-cycle oscillations.

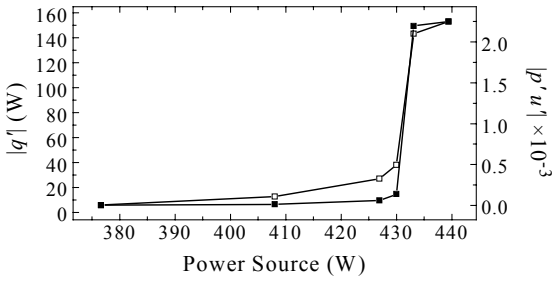

Fig. 7 Comparison between the modular product of acoustic pressure and velocity (–□–), and the modulus of heat oscillations (–■–).

the source (see Fig. 7). This key result confirms the arguments leading to Eqs. (17), (13), and (8).

In summary, large oscillations occur when the product of the velocity and pressure is large at the location of the heat source. They vanish when the product is zero or negative. This seems to agree with theoretical considerations presented in Sec. III. It appears that, when pressure and velocity are out of phase, oscillating fluid particles will be subjected to alternating pressure gradients that are continually unfavorable. This tends to suppress their motion and, thereby, the coupling with thermal oscillations at the heat source. These conclusions drawn speculatively are now confirmed numerically and experimentally. They seem to agree with the interpretation offered by Raun et al. regarding the effect of heat source location.[6] Accordingly, "maximum driving occurs at the point a quarter of the way from the bottom of the tube where the product of the acoustic velocity and acoustic pressure has the maximum magnitude." Although stated differently, their conclusions seem to agree with

our result requiring both pressure and velocity fluctuations to be present and to have additive amplitudes for driving to occur. They also match our experimental and numerical findings by confirming that "driving does not occur if the gauze is placed at either a velocity or pressure node."

VII. Conclusions

This paper extends our previous work that was devoted to a purely numerical simulation of the Rijke tube. The current investigation includes results from dimensional analysis and laboratory experiments which are supportive of previously reported results. They also lead to added insight into the physics of the problem.

The dimensional analysis is useful in providing several similarity parameters. In addition to geometric scaling ratios, these include the unsteady Euler, Eckert, Mach, and acoustic mode numbers. The scaling analysis is especially useful in revealing a thermoacoustic energy conversion parameter consisting of the ratio of fluctuating heat flux and energy flux vector modulus:

$$E_n = \frac{\overbrace{(q'/D^2)}^{\text{Fluctuating heat flux}}}{\underbrace{p'u'}_{\substack{\text{Acoustic energy flux} \\ \text{vector modulus}}}} \qquad (18)$$

Theoretically, this parameter was found to be an important characteristic of the acoustic motion in the Rijke tube. Numerical simulations were confirmatory.

In addition to dimensional analysis, the experimental study discussed in this paper furnishes an independent verification of the flow character. In agreement with previous observations, positioning of the heat source is found to be crucial for effective thermoacoustic coupling. For example, when the heat source is located at either pressure or acoustic nodes, no acoustic amplification is observed. The same can be said when the location corresponds to acoustic velocity and pressure of opposing signs. However, when the heat source is located at one-fourth the distance from the bottom, maximum sound pressure levels are recorded. This optimum position corresponds to a maximum product of acoustic pressure and velocity. When moving away from that point, a depreciation in the acoustic amplitude is noted. The experiment also indicates the importance of the air's mean flow convection currents in the coupling mechanism. It is found that, unless the air's mean flowrate is appreciable, no acoustic amplification can exist. Even when generated externally (via forced convection, for example), strong air currents can lead to acoustic growth. This was accomplished when the tube was either vertical or horizontal. Forced air currents can thus compensate for the lack of buoyancy in the horizontal configuration. Unsurprisingly, sealing the top drastically changes the wave character and suppresses acoustic excitation.

In this article, both empirical and numerical experiments were used to verify the role played by proper positioning of the heat source. In confirmation of our previous findings, it is concluded that 1) a minimum heat input is needed to trigger acoustic growth, 2) a critical heat input can lead to resonance, 3) a 45 degree phase difference exists between acoustic pressure and fluctuating heat flux, and 4) maximum acoustic amplification occurs when the product of acoustic velocity and pressure is maximum.

References

[1]Carrier, G. F., "The Mechanics of Rijke Tube," *Quarterly of Applied Mathematics,* Vol. 12, No. 4, 1955, pp. 383-395.

[2]Chu, B.-T., "Stability of Systems Containing a Heat Source -the Rayleigh Criterion," Research Memorandum Rept. 56D27, NACA, 1956.

[3]Miller, J., and Carvalho, J. A., "Comments on Rijke Tube," *Scientific American,* Vol. 204, No. 3, 1961, pp. 180-182.

[4]Maling, G. C., "Simplified Analysis of the Rijke Phenomenon," *Journal of the Acoustical Society of America,* Vol. 35, 1963, pp. 1058-1060.

[5]Zinn, B. T., "State of the Art Research Needs of Pulsating Combustion," Noise Control & Acoustics, ASME Paper 84-WA NCA-19, 1984.

[6]Raun, R. L., Beckstead, M. W., Finlinson, J. C., and Brooks, K. P., "Review of Rijke Tubes, Rijke Burners and Related Devices," *Progress in Energy & Combustion Science,* Vol. 19, No. 4, 1993, pp. 313-364.

[7]Entezam, B., Van Moorhem, W. K., and Majdalani, J., "Modeling of a Rijke-Tube Pulse Combustor Using Computational Fluid Dynamics," 33rd AIAA/ASME/SAE/ASEE Joint Propulsion Conference, Paper AIAA 97-2718, July 6-9, 1997.

[8]Feldman, K. T., "Review of the Literature on Rijke Thermoacoustic Phenomena," *Journal of Sound and Vibration,* Vol. 7, 1968, pp. 83-89.

[9]Feldman, K. T., "Review of the Literature on Soundhauss Thermoacoustic Phenomena," *Journal of Sound and Vibration,* Vol. 7, 1968, pp. 71-82.

[10]Bai, T., Cheng, X. C., Daniel, B. R., Jagoda, J. I., and Zinn, B. T., "Performance of a Gas Burning Rijke Pulse Combustor with Tangential Reactants Injection," *Combustion Science & Technology,* Vol. 94, No. 1-6, 1993, pp. 1-10.

[11]Wall, T. F., Bhattacharya, S. P., Baxter, L. L., Richards, G., and Harb, J. N., "Character of Ash Deposits and the Thermal Performance of Furnaces," *Fuel Processing Technology,* Vol. 44, No. 1-3, 1995, pp. 143-153.

[12]Reiner, D., Xu, Z. X., Su, A., Bai, T., Daniel, B. R. *et al.*, "Combustion of Heavy Liquid Fuels in a Rijke Type Pulse Combustor," Combustion Instabilities Driven by Thermo-Chemical Acoustic Sources, ASME Paper NCA 4, 1989.

[13]Wang, M.-R., and Zinn, B. T., "Performance Characteristics of a Prototype, Rijke Type Pulsating Combustor," *Journal of the Chinese Society of Mechanical Engineers,* Vol. 8, No. 5, 1987, pp. 339-345.

[14]Yavuzkurt, S., Ha, M. Y., Koopmann, G., and Scaroni, A. W., "Model of the Enhancement of Coal Combustion Using High-Intensity Acoustic Fields," *Journal of Energy Resources Technology-Transactions of the ASME,* Vol. 113, No. 4, 1991, pp. 277-285.

[15]Stewart, C. R., Lemieux, P. M., and Zinn, B. T., "Application of Pulse Combustion to Solid and Hazardous Waste Incineration," *Combustion Science & Technology,* Vol. 94, No. 1-6, 1993, pp. 427-446.

[16]Morris, G. J., Welter, M. J., and Richards, G. A., "Investigation of Pulse-Combustor Design for Slurry Atomization," Fossil Fuel Combustion Symposium - Presented at the Thirteenth Annual Energy-Sources Technology Conference and Exhibition, Petroleum Division, ASME Paper PD 30, 1990.

[17]Hoffman, T. L., and Koopmann, G. H., "Visualization of Acoustic Particle Interaction and Agglomeration: Theory Evaluation," *Journal of the Acoustical Society of America,* Vol. 101, No. 6, 1997, pp. 3421-3429.

[18]Hoffmann, T. L., Chen, W., Koopmann, G. H., Song, L., and Scaroni, A. W., "Experimental and Numerical Analysis of Bimodal Acoustic Agglomeration," ASME Winter Annual Meeting, ASME Paper 91-WA-NCA-5, 1991.

[19]Hoffmann, T. L., and Koopmann, G. H., "New Technique for Visualization of Acoustic Particle Agglomeration," *Review of Scientific Instruments,* Vol. 65, No. 5, 1994, pp. 1527-1536.

[20]Miller, N., Powell, E. A., Chen, F., and Zinn, B. T., "Use of Air Staging to Reduce the Nox Emissions from Coal Burning Rijke Pulse Combustors," *Combustion Science & Technology,* Vol. 94, No. 1-6, 1993, pp. 411-426.

[21]Reethof, G., "Acoustic Agglomeration of Power Plant Fly Ash for Environmental and Hot Gas Clean-Up," *Journal of Vibration & Acoustics-Transactions of the ASME,* Vol. 110, No. 4, 1988, pp. 552-557.

[22]Reethof, G., Koopmann, G. H., and Dorchak, T., "Acoustic Agglomeration for Particulate Control at High Temperatures and High Pressure. Some Recent Results," ASME Winter Annual Meeting, ASME Paper WA/NCA4, 1989.

[23]Sharifi, R., Miller, S. F., Scaroni, A. W., Koopmann, G. H., and Chen, W., "In Situ Monitoring of the Acoustic Agglomeration of Fly Ash Particles," ASME, International Gas Turbine Institute, Paper 9, 1994.

[24]Song, L., Koopmann, G. H., and Hoffmann, T. L., "Improved Theoretical Model of Acoustic Agglomeration," *Journal of Vibration & Acoustics-Transactions of the ASME,* Vol. 116, No. 2, 1994, pp. 208-214.

[25]Tiwary, R., and Reethof, G., "Effect of Hydrodynamic Interaction between Small Particles on Fillup of Agglomeration Volume in Acoustic Agglomeration of Aerosols," Presented at the ASME Winter Annual Meeting, ASME Paper 87-WA/NCA-4, 1987.

[26]Tiwary, R., and Reethof, G., "Numerical Simulation of Acoustic Agglomeration and Experimental Verification," *Journal of Vibration & Acoustics Transactions of the ASME,* Vol. 109, No. 2, 1987, pp. 185-191.

[27]Bai, T., Cheng, X. C., Daniel, B. R., Jagoda, J. I., and Zinn, B. T., "Vortex Shedding and Periodic Combustion Processes in a Rijke Type Pulse Combustor," *Combustion Science & Technology,* Vol. 94, No. 1-6, 1993, pp. 245-258.

[28]Carvalho, J. A., Miller, N., Daniel, B. R., and Zinn, B. T., "Combustion Characteristics of Unpulverized Coal under Pulsating and Non-Pulsating Conditions," *Fuel,* Vol. 66, No. 1, 1987, pp. 4-8.

[29]George, W., and Reethof, G., "On the Fragility of Acoustically Agglomerated Submicron Fly Ash Particles," *Journal of Vibration, Acoustics, Stress, and Reliability in Design,* Vol. 108, 1986, pp. 332-329.

[30]Chen, T. Y., Hegde, U. G., Daniel, B. R., and Zinn, B. T., "Flame Radiation and Acoustic Intensity Measurements in Acoustically Excited Diffusion Flames," *Journal of Propulsion & Power,* Vol. 9, No. 2, 1993, pp. 210-216.

[31]Wang, M.-R., and Zinn, B. T., "Controlling Processes in Rijke Type Coal Burning Pulsating Combustors," *Chemical and Physical Processes in Combustion,* Vol. 61, 1984, pp. 1-61.

[32]Zinn, B. T., "Pulse Combustion: Recent Applications and Research Issues," Proceedings of the 24th International Symposium On Combustion, Combustion Institute Paper 19626, 1992.

[33]Reuter, D., Daniel, B. R., Jagoda, J., and Zinn, B. T., "Periodic Mixing and Combustion Processes in Gas Fired Pulsating Combustors," Western States Section, Combustion Institute, Paper 14, 1985.

[34]Xu, Z. X., Reiner, D., Su, A., Bai, T., Daniel, B. R. *et al.*, "Flame Stabilization and Combustion of Heavy Liquid Fuels in a Rijke Type Pulse Combustor," Fossil Fuel Combustion, ASME, Petroleum Division Paper PD 33, 1991.

[35]Richards, G. A., Logan, R. G., Meyer, C. T., and Anderson, R. J., "Ash Deposition at Coal-Fired Gas Turbine Conditions: Surface and Combustion Temperature Effects," *Journal of Engineering for Gas Turbines & Power-Transactions of the ASME,* Vol. 114, No. 1, 1992, pp. 132-138.

[36]Richards, G. A., Morris, G. J., Shaw, D. W., Keeley, S. A., and Welter, M. J., "Thermal Pulse Combustion," *Combustion Science & Technology,* Vol. 94, No. 16, 1993, pp. 57-85.

[37]Yavuzkurt, S., Ha, M. Y., Reethof, G., Koopmann, G., and Scaroni, A. W., "Effect of an Acoustic Field on the Combustion of Coal Particles in a Flat Flame Burner," *Journal of Energy Resources Technology-Transactions of the ASME,* Vol. 113, No. 4, 1991, pp. 286-293.

[38]Lieuwen, T., and Zinn, B. T., "Role of Equivalence Ratio Oscillations in Driving Combustion Instabilities in Low Nox Gas Turbines," *Symposium (International) on Combustion,* Vol. 2, 1998, pp. 1809-1816.

[39]Tiwary, R., and Reethof, G., "Hydrodynamic Interaction of Spherical Aerosol Particles in a High Intensity Acoustic Field," *Journal of Sound and Vibration,* Vol. 108, 1986, pp. 33-49.

[40]Hegde, U. G., Reuter, D., Daniel, B. R., and Zinn, B. T., "Experimental Investigations of Combustion Instabilities in Ramjets," Chemical and Physical Processes in Combustion, Paper 60, 1985.

[41]Price, E. W., "Review of Combustion Instability Characteristics of Solid Propellants," AGARD Conference Proceedings, Technivision Services Paper 1, 1968.

[42]Zinn, B. T., Miller, N., A, C. J., and R, D. B., "Pulsating Combustion of Coal in a Rijke Type Combustor," Proceedings of the 19th International Symposium on Combustion,, 1982.

[43]Hirt, C. W., and Nichols, B. D., "Volume of Fluid (Vof) Method for the Dynamics of Free Boundaries," *Journal of Computational Physics,* Vol. 39, 1981, pp. 201-225.

[44]Flow-3D, Flow-Science Incorporated, Los Alamos, New Mexico, 1997.

[45]Carvalho, J. A., Ferreira, C., Bressan, C., and Ferreira, G., "Definition of Heater Location to Drive Maximum Amplitude Acoustic Oscillations in a Rijke Tube," *Combustion and Flame,* Vol. 76, No. 1, 1989, pp. 17-27.